Revue des Composites et des Matériaux Avancés-Journal of Composite and Advanced Materials
Vol. 36, No. 1, February, 2026, pp. 155-163
Journal homepage: http://iieta.org/journals/rcma

# Synergistic Enhancement of Sulfate-Resistant Polymer Repair Concrete Incorporating Supplementary Cementitious Materials and Polypropylene Fibers

Mohammed H. Majid*, Jasim M. Abed

Department of Building and Construction Engineering Techniques, Engineering Technical College, Northern Technical University, Mosul 41002, Iraq

Corresponding Author Email: Mohamed.h.atim@ntu.edu.iq



https://doi.org/10.18280/rcma.360115

**Received:** 4 September 2025
**Revised:** 21 November 2025
**Accepted:** 16 February 2026
**Available online:** 28 February 2026

***Keywords:***
*high-performance concrete, polymer-modified concrete, repair materials, supplementary cementitious materials, silica fume, ground granulated blast furnace slag, polypropylene fibers, sulfate resistance, slant shear bond, synergistic effect*

**ABSTRACT**

Concrete structures in sulfate-aggressive environments frequently experience rapid deterioration, necessitating durable and cost-effective repair solutions. The objective of this study is to develop a high-performance polymer repair concrete (HPPRC) tailored for aggressive sulfate conditions. Sulfate-resistant cement replaced ordinary Portland cement to address chemical attack, while silica fume and ground granulated blast furnace (GGBS) were incorporated as supplementary cementitious materials (SCMs) to enhance pozzolanic activity. Polymer and polypropylene fibers were also introduced to improve bonding performance, durability, and crack resistance. Eighteen distinct mix combinations were designed with varying proportions of polymer and SCMs, while keeping fiber dosage constant. These mixes were tested for slump, water absorption, flexural strength, and slant shear bond performance. The results indicated that the integration of SCMs with polymer modification significantly improved mechanical strength and durability. In particular, mixes containing higher levels of silica fume and GGBS combined with moderate polymer content exhibited enhanced strength development, reduced permeability, and superior bond resistance. The improved performance can be attributed to synergistic effects of pozzolanic reactions, polymer adhesion, and fiber reinforcement in controlling cracks. Overall, the study demonstrates that strategically combining sulfate-resistant cement, polymer, fibers, and SCMs can yield highly effective repair systems for sustainable rehabilitation of concrete exposed to sulfate environments.

## 1. INTRODUCTION

Concrete remains the most widely used construction material due to its strength, versatility, and affordability. However, the deterioration of aging infrastructure, particularly in sulfate-rich environments, poses serious durability and safety challenges. Conventional cement-based repair materials often fail to provide long-term performance under such aggressive conditions, highlighting the need for advanced, durable, and sustainable repair solutions [1].

Recent advances have demonstrated that polymer incorporation into cementitious systems significantly improves bonding, crack resistance, and resistance to chemical attack [2]. Polymer-modified concrete (PMC) and polymer-cement composites exhibit enhanced durability under harsh exposure conditions [3]. At the same time, supplementary cementitious materials (SCMs) such as silica fume and ground granulated blast furnace (GGBS) refine the pore structure, reduce permeability [4], and support sustainability through reduced cement demand and the reuse of industrial by products [5]. Several studies have investigated polymers or SCMs individually; however, limited research has explored their combined use with fibers to create high-performance repair concrete tailored for sulfate-rich environments [6]. This gap restricts the development of reliable repair guidelines for modern infrastructure.

To address this gap, the present study systematically examines the synergistic and complementary effects of SCMs, polymer, and polypropylene fibers on repair concrete. The objectives are to:

1. Analyze material interactions and their influence on microstructural refinement, 2. Evaluate compressive, flexural, and bond strength as well as water absorption, and 3. Propose optimized mixture designs that balance sustainability with superior performance. The findings provide practical insights and implementation strategies for durable repair systems suitable for aggressive sulfate conditions.

## 2. EXPERIMENTAL PROGRAM AND MATERIALS

### 2.1 Cement

Sulfate-Resistant Portland Cement, often referred to as

Type V cement under ASTM C150 [7] classification, was selected with a sense of caution and expectation. This wasn't a casual choice. The exposure conditions demanded something capable of withstanding harsh sulfate attack, a threat all too common in aggressive soil and groundwater environments. Type V cement, known for its low tricalcium aluminate ($C_3A$) content, was the logical answer product of both chemistry and necessity. Table 1 outlines the physical and chemical properties of the cement used, all verified according to ASTM C150.

**Table 1.** Physical and chemical properties of Sulfate-resistant Portland cement

| Property | Results | ASTM C150 Limit (type v) |
|---|---|---|
| Fineness (Blaine), m²/kg | 350 | Min. 320 |
| Soundness (autoclave expansion), % | 0.051 | Max. 0.80 |
| Setting time (Initial), minutes | 115 | Min. 45 |
| Compressive strength (3 days), MPa | 24.7 | — |
| Compressive strength (7 days), MPa | 36.5 | — |
| Loss on ignition (LOI), % | 1.45 | Max. 3.0 |
| Insoluble residue, % | 0.44 | Max. 0.75 |
| Magnesium oxide (MgO), % | 2.1 | Max. 6.0 |
| Sulfur trioxide ($SO_3$), % | 2.11 | Max. 2.3 |
| Tricalcium aluminate ($C_3A$), % | 3.8 | Max. 5.0 |

**Table 2.** Physical and chemical properties of ground granulated blast furnace (GGBS)

| Property | Results | ASTM C989 Requirement [8] |
|---|---|---|
| Specific gravity | 2.8 | — |
| Fineness (Blaine), m²/kg | 466 | ≥ 275 |
| Glass content, % | 96 | — |
| Moisture content, % | 0.7 | — |
| Loss on ignition (LOI), % | 0.42 | ≤ 3.0 |
| Calcium oxide (CaO), % | 41.3 | — |
| Silicon dioxide ($SiO_2$), % | 36.8 | — |
| Aluminum oxide ($Al_2O_3$), % | 13.3 | — |
| Magnesium oxide (MgO), % | 10.2 | ≤ 18.0 (ASTM C989) |
| Sulfur trioxide ($SO_3$), % | 3.1 | ≤ 4.0 |
| Chloride content ($Cl^-$), % | 0.015 | ≤ 0.05 |
| Activity index (7 days), % of OPC | 77 | ≥ 75 (grade 100) |
| Activity index (28 days), % of OPC | 98.3 | ≥ 95 (grade 100) |

### 2.2 Ground granulated blast furnace slug

It was used in this study as a partial replacement for Portland cement to enhance the durability and long-term performance of the mixtures. GGBS is a fine, gray-black powder obtained by rapidly cooling molten iron slag from blast furnaces and then grinding it into a cement-like material. Its primary role in this research was to improve the sulfate resistance, reduce the heat of hydration, and contribute to the overall strength development of the cementitious matrix over time. The GGBS used conformed to ASTM C989 [8] requirements, indicating moderate reactivity. It had a specific surface area of approximately 466 m²/kg, which supported its hydraulic activity when blended with cement. Table 2 outlines the physical and chemical properties of the GGBS used. Figure 1 shows the GGBS during the grinding and refining process.

### 2.3 Silica fume

A highly reactive pozzolanic material with ultrafine particles was used to enhance the microstructure of the cement matrix (as shown in Figure 2). Its high $SiO_2$ content promotes secondary hydration, forming additional C-S-H gel that refines pores and improves durability. These micro-level effects significantly boost the performance of high-performance concrete. The typical composition is shown in Table 3.

**Figure 1.** Ground granulated blast furnace slug (GGBS)


**Figure 2.** The used ultrafine particles of silica fume

**Table 3.** Chemical composition and physical properties of silica fume

| $SiO_2$ | $Al_2O_3$ | $Fe_2O_3$ | CaO | MgO | $SO_3$ | $Na_2O$ | $K_2O$ | LOI | Specific Gravity | Blaine (cm²/g) |
|---|---|---|---|---|---|---|---|---|---|---|
| 95.9 | 0.22 | 0.13 | 0.45 | 0.56 | - | 0.23 | 0.72 | 1.93 | 2.25 | 19,350 |

NOTE: Loss on ignition (LOI)

### 2.4 Polymer (Sikadur 31)

In this study, Sikadur 31, a high-performance polymer adhesive supplied by Sika Construction in Istanbul, Turkey, was used as a key bonding agent according to ASTM C881 [9]. This material arrives in two components, Part A and Part B, which must be combined in a precise ratio as specified in the technical datasheet. Once mixed, the blend cures quickly, developing significant early strength and forming a dense, highly adhesive paste. Its use in this research was deliberate. With its proven record in structural repair and anchoring, Sikadur 31 provided the mechanical reliability and chemical stability needed to ensure strong adhesion across interfaces. The main physical and mechanical properties of the polymer are presented in Table 4, while its commercial packaging is shown in Figure 3.

**Table 4.** Physical and chemical properties of polymer (Sikadur 31)

| Property | Results | ASTM C881 [8] Requirement |
|---|---|---|
| Type | Type I / IV | Type i: bonding adhesive, type iv: structural bonding |
| Grade | Grade 3 (paste) | Grade 3: gel or paste |
| Class | Class C | Class C: use at temperatures 4-16°C |
| Mix ratio (A: B, by weight) | 2:1 | As specified by manufacturer |
| Pot life (200 g @ 20°C) | 50 minutes | ≥ 30 minutes (typical for Class C) |
| Tensile strength (7 days) | 32.7 MPa | ≥ 30 MPa for type iv |
| Elongation at break | 3% | 1-5% |
| Compressive strength (7 days) | 77.4 MPa | ≥ 70 MPa (for structural applications) |
| Bond strength to concrete | 16.8 MPa | ≥ 10 MPa (moist-cured concrete) |
| Water absorption (24 hrs) | 0.11% | ≤ 1.0% |
| Thermal compatibility | Pass | No delamination or cracking |

**Figure 3.** The used polymer (Sikadur 31)

### 2.5 Polypropylene fibers

Polypropylene fibers conforming to ASTM C1116 [10] were incorporated into the concrete mix at a dosage of 0.2% by volume. Each fiber had a length of 10 mm and a nominal diameter of approximately 18 microns, a size selected to strike a balance between effective crack-bridging and uniform dispersion within the cementitious matrix. These synthetic fibers were introduced not to increase strength in the traditional sense, but to control plastic shrinkage, reduce microcracking, and enhance post-cracking behavior. The detailed physical and chemical characteristics of the polypropylene fibers are presented in Table 5.

**Table 5.** Physical and chemical properties of polypropylene fibers

| Property | Results |
|---|---|
| Material type | Isotactic polypropylene |
| Form | Monofilament |
| Fiber length | 10 mm |
| Fiber diameter | 18 µm |
| Specific gravity | 0.91 g/cm³ |
| Tensile strength | 500 MPa |
| Elastic modulus | 4.2 GPa |
| Melting point | 165°C |
| Water absorption | Nil |
| Alkali resistance | Excellent |
| Acid resistance | Good |
| Color | Natural white or grey |

### 2.6 Fine aggregate

For fine aggregate, natural river sand was carefully selected and sourced directly from quarries along the Tigris River. Extensive testing confirmed that this sand conformed precisely to Zone 4 grading criteria, making it exceptionally suitable for PMC applications. Specific gravity testing yielded a value of about 2.62. The absorption percentage was 1.2%, with a moisture content 0.5%. The aggregate's gradation was meticulously verified to align with ASTM C33 [11] standards, as detailed clearly in Figure 4.

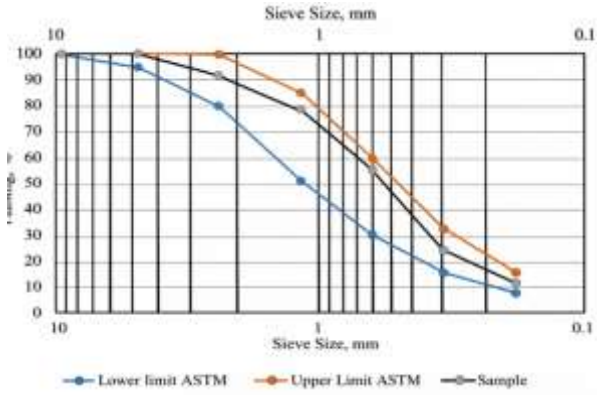


**Figure 4.** Gradation of fine aggregate used

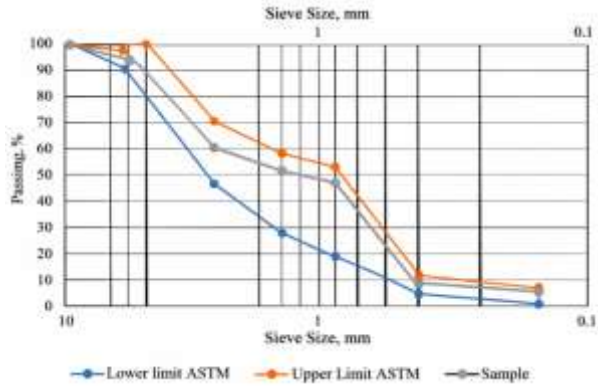


**Figure 5.** Gradation of coarse aggregate used

### 2.7 Coarse aggregate

The coarse aggregate selected after careful consideration was sourced directly from the crushed river gravel of Tigris River quarries. With a maximum aggregate size of 19.5 mm, it wasn't merely chosen by coincidence; rather, the suitability for PMC dictated this specific size range. Determining the aggregate's specific gravity of 2.73, typical and reassuringly acceptable for structural concrete use. The water absorption rate 0.8%, and the moisture content 0.4%. Furthermore, aggregate gradation meticulously followed the guidelines specified by ASTM C33 [11], as precisely detailed in Figure 5.

## 3. MIX PROPORTIONS

Concrete mixes were produced following the designed proportions as shown in Table 6. A high-range water-reducing admixture (superplasticizer) was used at a fixed ratio of 1% of the binder weight to achieve the desired workability. Materials were mixed consistently, ensuring uniform fiber distribution and homogeneous integration of polymer.

**Table 6.** Mix proportions of polymerized repair concrete

| Mix ID | Cement ($kg/m^3$) | Silica Fume (%) | GGBS (%) | Polymer (%) | Polypropylene Fibers (%) | Fine Aggregate ($kg/m^3$) | Coarse Aggregate ($kg/m^3$) | W/B |
|---|---|---|---|---|---|---|---|---|
| M0 | 450 | ---- | ---- | ---- | ---- | 713 | 1046 | 0.46 |
| M1 | 382.5 | 5% | 10% | 5% | 0.2% | 713 | 1046 | 0.46 |
| M2 | 337.5 | 5% | 20% | 5% | 0.2% | 713 | 1046 | 0.46 |
| M3 | 292.5 | 5% | 30% | 5% | 0.2% | 713 | 1046 | 0.46 |
| M4 | 360 | 10% | 10% | 5% | 0.2% | 713 | 1046 | 0.46 |
| M5 | 315 | 10% | 20% | 5% | 0.2% | 713 | 1046 | 0.46 |
| M6 | 270 | 10% | 30% | 5% | 0.2% | 713 | 1046 | 0.46 |
| M7 | 337.5 | 15% | 10% | 5% | 0.2% | 713 | 1046 | 0.46 |
| M8 | 292.5 | 15% | 20% | 5% | 0.2% | 713 | 1046 | 0.46 |
| M9 | 247.5 | 15% | 30% | 5% | 0.2% | 713 | 1046 | 0.46 |

## 4. RESEARCH METHODOLOGY

This study employed concrete mixes carefully designed in strict accordance with the proportions detailed in Table 6. The base binder was sulfate-resistant cement, partially replaced with silica fume (5%, 10%, 15%) and GGBS (10%, 20%, 30%), while polymer was added at 5% or 10% as a polymer modifier. Polypropylene fibers (0.2% by volume) were uniformly dispersed to prevent clustering. A fixed water-to-binder ratio of 0.46 was maintained for all mixes, with superplasticizer added at 1% by binder mass to ensure adequate workability. Specimens were cast into standardized molds to facilitate consistent comparison:

All concrete mixes were prepared in a pan mixer using a standardized sequence: cement, silica fume, and GGBS were first dry-blended for 2 minutes, aggregates were then added and mixed for another 2 minutes, and finally polypropylene fibers (0.2% by volume), Sikadur 31 polymer (pre-mixed at 2:1 ratio of Part A: Part B as per ASTM C881 and manufacturer's guidelines), superplasticizer (1% by binder weight), and water were gradually introduced, with mixing continued for 3 minutes until homogeneity was achieved. Specimens were cast in standard molds, demolded after 24 hours, and cured in water at 20 ± 2°C and relative humidity above 95%, while polymer-modified samples were first cured at laboratory conditions for 24 hours before immersion. The polymer was applied within its pot life (50 minutes at 20°C) to ensure bonding reliability. For each mix, six specimens were prepared for each compressive, flexural, and slant shear tests, providing three replicates at each age (28 and 90 days); this sample size was selected to balance statistical reliability with resource efficiency. A schematic flowchart (Figure 6) summarizes the overall experimental program from materials preparation through mixing, curing, and mechanical and durability testing.

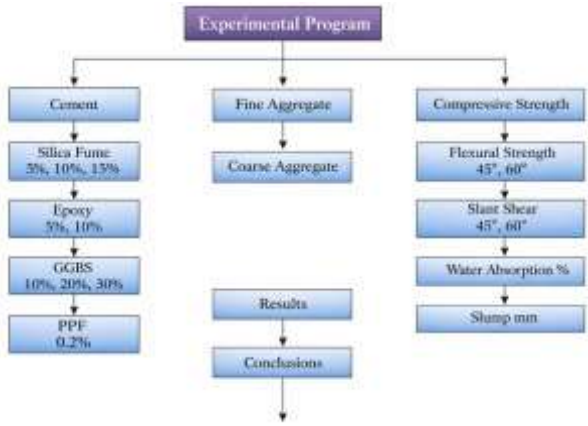


**Figure 6.** Flowchart of the experimental program

The slump test was conducted in accordance with ASTM C143 [12] to evaluate theworkability of fresh concrete. The test procedure involved filling a standard slump cone mold in three equal layers, with each layer compacted using 25 blows of a tamping rod. After the mold was lifted vertically, the slump was measured as the vertical subsidence of the concrete. Compressive strength was determined using 100 mm cubic specimens in accordance with BS EN 12390-3 [13]. For each mixture, six specimens were prepared, of which three were tested under standard curing conditions. The compressive load was applied at a controlled loading rate of 0.6 MPa/s. The specimens were cast with inclined contact surfaces at 90° as part of a modified compression testing configuration. Flexural strength testing was performed following ASTM C78 [14] using prismatic specimens with dimensions of 100 × 100 × 400 mm, as illustrated in Figure 7. A total of six specimens were prepared for each mixture, and the applied loading rate was maintained at 0.06 MPa/s. To

investigate the influence of interface inclination on flexural behavior, half of the specimens were prepared with a 60° inclined surface, while the remaining specimens had a 45° inclination.

**Figure 7.** Sample utilized in the flexural strength test

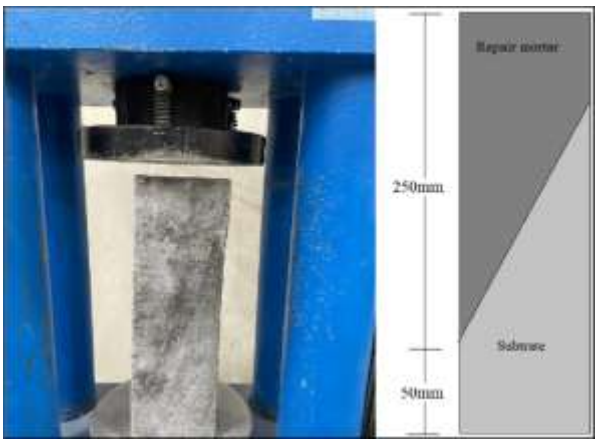


**Figure 8.** Sample utilized in the slant-shear test

Following ASTM C882 [15], the slant shear prisms were performed with a loading rate of 0.6 MPa/min. Another set of six per mix as shown in Figure 8. These were divided between 30° and 60° bond angles, specifically designed to test shear performance at the interface. To assess porosity and potential durability, the water absorption test was conducted as per ASTM C642 [16]. Oven-dried specimens were weighed, submerged in water, and reweighed after saturation. The percentage of absorbed water provided insight into the internal pore structure, directly reflecting the concrete's resistance to long-term deterioration due to moisture ingress. Each test aimed to provide critical insights into the mechanical and durability behavior of PMC, especially the interactions between polymer, SCMs, and fibers. The methodology, summarized in Figure 6, underpinned a broader effort to uncover synergies and performance trends in high-performance repair concretes.

## 5. RESULTS AND DISCUSSION

### 5.1 Slump test

The workability of the fresh concrete mixes, as shown in Figure 9 for (M1 to M9) was assessed using the slump test, following the standard procedure outlined in ASTM C143/C143M [12]. For each mix, a fresh concrete sample was prepared and poured into a standard slump cone in three layers. Each layer was tamped 25 times using a standard tamping rod to ensure uniform compaction. After filling, the cone was slowly lifted vertically, and the decrease in the height of the concrete (slump) was measured immediately. The slump values recorded for all mixes fell within the 11.1 cm to 12.6 cm range, which is considered moderate and appropriate for repair applications requiring good workability without segregation or bleeding. However, the results of the slump are illustrated in Figure 10.

**Figure 9.** Slump test of polymer concrete

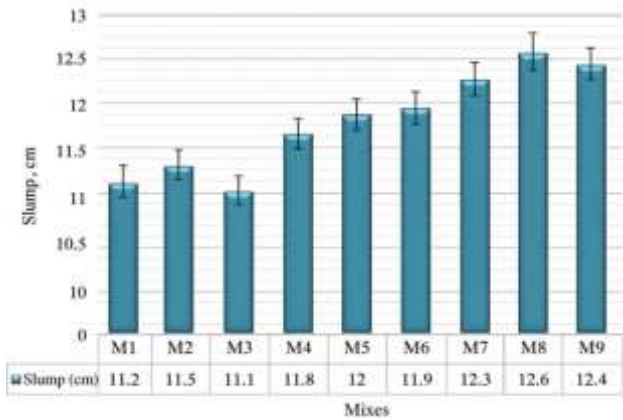


**Figure 10.** Results of the polymer concrete slump test

The lowest slump values were observed for mixtures M3 (11.1 cm) and M1 (11.2 cm). These mixtures contained lower proportions of SCMs, which resulted in reduced fines content and consequently a stiffer fresh concrete consistency. As the contents of silica fume and GGBS increased, as observed in mixtures M7 to M9, a gradual increase in slump was recorded. The maximum slump value of 12.6 cm was achieved for mixture M8. This improvement can be attributed to enhanced particle packing, improved paste cohesiveness, and the lubricating effect of the polymer modifier. Although the incorporation of 0.2% polypropylene fibers generally tends to reduce workability due to fiber-induced water retention and restricted flow, all mixtures maintained acceptable workability levels. This indicates that the selected water-to-binder ratio and superplasticizer dosage were sufficient to offset the workability reduction associated with fiber addition.

The moderate slump values achieved across all mixtures ensured adequate flowability for placement and consolidation

while minimizing the risk of segregation. Such characteristics are particularly important for repair applications, where proper surface finishing, interfacial bonding, and long-term durability are critical.

### 5.2 Water absorption

To fully understand, or perhaps more realistically, attempt to understand the water absorption characteristics of the developed PMC mixtures (M1-M9), the absorption test was rigorously conducted. Porosity and permeability, undeniably critical yet inherently ambiguous characteristics, were evaluated strictly according to the procedures outlined in ASTM C642 [16]. For each mixture, three cubic specimens (100 mm × 100 mm × 100 mm) were prepared and cured underwater for 28 days. After curing, the samples were carefully removed from their immersion environment and gently surface-dried at ambient room conditions for precisely 24 hours. To achieve certainty, or at least to approach it more confidently, further drying was performed in a controlled oven environment at 100 ± 5℃. This drying phase lasted 24 hours and was continued meticulously until a constant mass was achieved. Once cooled thoroughly in a desiccator, ensuring no reabsorption of atmospheric moisture, this stable dry mass (A) was carefully recorded. Subsequently, the specimens were immersed again, this time at room temperature, for 48 hours. After this period, they were removed, wiped, and weighed to obtain the saturated mass (B). Finally, the ultimate saturated mass post-boiling (C) was determined and carefully documented.

Water absorption percentages were calculated according to the Eq. (1):

$$Water\ absorption\ \% = \frac{C - A}{A} \times 100 \qquad (1)$$

For each mix, average values from the three tested samples were reported clearly and systematically in Figure 11.

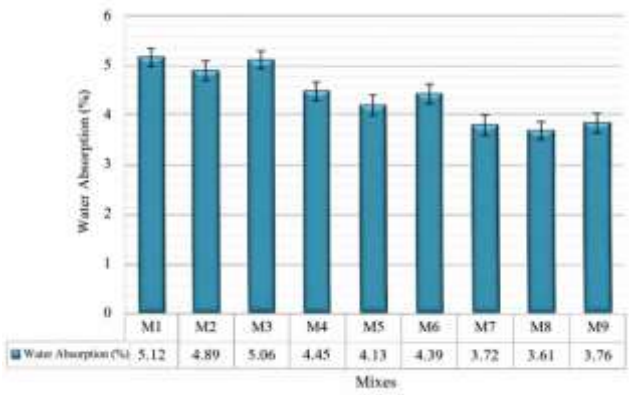


**Figure 11.** Water absorption of polymer concrete

The water absorption values varied between 5.12% and 3.61%, indicating a gradual but meaningful reduction in porosity across the mix series. The general trend suggests that increasing the dosage of SCMs and integrating polymer contributed to the refinement of the microstructure and improved resistance to water ingress. The highest absorption was observed in M1 (5.12%) and M3 (5.06%), both of which had lower SCM content and represent the baseline performance of the system. These relatively high absorption values reflect a more open pore structure, typical of mixes without optimized particle packing or secondary hydration reactions. The limited polymer and pozzolanic contribution in these mixes likely led to capillary continuity and higher water uptake. Additionally, minor surface voids and inconsistent compaction may have contributed to these elevated values factors not uncommon in site or lab repair conditions. In contrast, M8 (3.61%), M7 (3.72%), and M9 (3.76%) showed the lowest water absorption. These mixes contained higher levels of silica fume and GGBS, which enhanced pozzolanic reactivity and reduced capillary porosity. The polymer likely filled part of the pore network and created a partial hydrophobic barrier, consistent with observations in previous studies [17, 18]. However, even in these well-optimized mixes, the absorption did not drop below 3.6%, indicating that total elimination of porosity is not practical and is influenced by curing efficiency, mixing energy, and air content. Intermediate mixes such as M4 to M6 showed reasonable values (4.13-4.45%), reflecting a balanced design. Slight variations in absorption among them may be attributed to inconsistencies in curing temperature, mix homogeneity, or fiber distribution, all of which can affect the interconnected porosity and therefore the absorption result. The absorption test results confirm that higher SCM content combined with polymer resin improves impermeability, but field-relevant variability in results remains due to practical factors like compaction, surface finish, and fiber orientation. This highlights the importance of mix optimization and quality control, particularly when designing repair mortars for durability in aggressive exposure conditions.

### 5.3 Compressive strength

The compressive strength results of mixes M1 to M9, illustrated in Figure 12, show a clear and progressive enhancement in strength from 28 days to 90 days, which is typical in blended cementitious systems where continued hydration and pozzolanic reactions contribute to long-term performance. All mixes exhibit strength development over time, with an average increase of approximately 2.5-3.2 MPa, indicating the ongoing contribution of SCMs. The lowest performance was recorded in M1 and M3, which contained minimal SCM content, indicating limited refinement of pore structure and reduced secondary hydration. This aligns with the study [17], which reported that polymer modification alone provides limited strength improvement without the synergistic effect of reactive mineral admixtures.

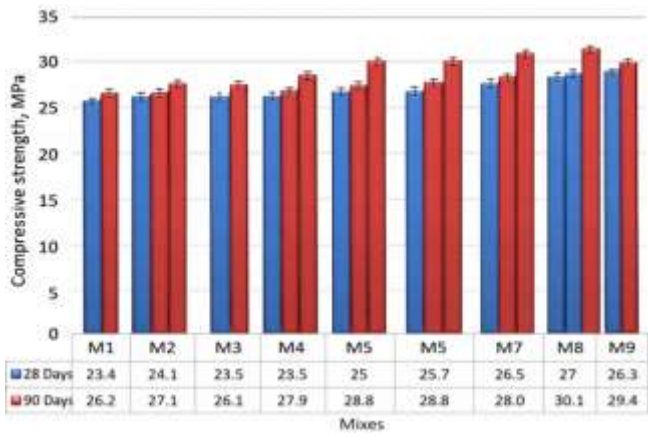


**Figure 12.** Compressive strength of polymer concrete

In contrast, M8 achieved the highest compressive strength (30.1 MPa at 90 days), followed by M7 and M9. This superior performance can be attributed to the higher silica fume and GGBS content, which refined the pore structure and generated additional calcium silicate hydrate (C-S-H), thereby densifying the matrix. The inclusion of polymer (5%) improved bonding at the interface, while polypropylene fibers (0.2%) provided crack-bridging and stress redistribution. These microstructural mechanisms are supported by Guo et al. [18] and Shill et al. [19], who observed enhanced cohesion and reduced microcracking when polymer and fibers were combined with SCMs.

Intermediate mixes (M4-M6) showed moderate improvements (28 MPa), reflecting the incremental role of SCMs in strengthening the matrix. Overall, the results confirm that the integration of SCMs with polymer and fibers promotes microstructural refinement, reduced porosity, and enhanced internal cohesion, producing a synergistic improvement in compressive strength compared to conventional repair concretes.

### 5.4 Flexural strength

The flexural strength results illustrated in Figure 13 for mixes M1 through M9 indicate a consistent and progressive improvement from 28 to 90 days, with strength gains ranging between 0.4 MPa to 0.5 MPa across all mixes. This trend reflects the continuous hydration of cementitious materials and the beneficial role of polymer in enhancing tensile stress resistance and crack-bridging capacity within the concrete matrix. According to the study [18], the lowest values were observed in M1 and M3 (3.51 and 3.93 MPa at 28 and 90 days, respectively), which can be attributed to their limited SCM content, resulting in weaker pozzolanic activity and reduced refinement of the interfacial transition zone (ITZ). Such behavior is consistent with findings by the study [12], who emphasized that a polymer alone cannot significantly enhance tensile properties without reactive mineral admixtures.

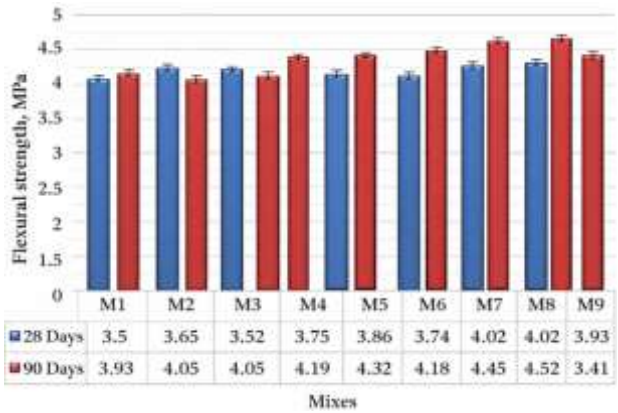


**Figure 13.** Flexural strength of polymer concrete

In contrast, M8 achieved the highest flexural strength (4.52 MPa at 90 days), followed by M7 (4.45 MPa) and M9 (3.41 MPa). This superior performance can be explained by the optimized synergy between silica fume, GGBS, and polymer, which improved particle packing, densified the ITZ, and promoted additional C-S-H formation. Polymer contributed to micro-level adhesion, distributing tensile stresses more evenly across the matrix, while polypropylene fibers (0.2%) acted as crack arresters and enhanced post-cracking toughness. These mechanisms are supported by Shill et al. [19] and Liang et al. [20], who reported that combining polymers with SCMs and fibers significantly improves resistance to crack propagation under flexural loading.

Intermediate mixes (M4-M6) exhibited moderate improvements (4.18-4.32 MPa at 90 days), confirming that incremental SCM dosage and polymer inclusion lead to steady enhancements in tensile performance [21]. Overall, the combined effect of SCMs, polymer, and fibers produced a denser, more cohesive microstructure with improved crack-bridging and energy absorption capacity, distinguishing the optimized mixes from conventional repair concretes [22].

### 5.5 Slant shear bond strength

The slant shear strength results, as illustrated in Figure 14 for the repair concrete mixes M1 to M9, demonstrate a consistent and notable improvement from 28 to 90 days, emphasizing the progressive development of bond strength at the interface between the repair material and the existing substrate. This enhancement is largely attributed to the combined effect of SCMs and polymer, which synergistically improve both the microstructure and adhesion characteristics of the matrix.

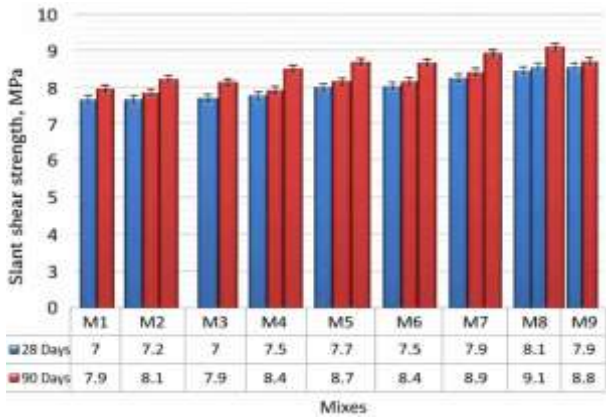


**Figure 14.** Slant shear strength of concrete

The lowest bond strengths were recorded in M1 and M3 (7.0 MPa at 28 days, 7.9 MPa at 90 days), reflecting their limited SCM content and correspondingly weaker pozzolanic reactivity, which restricted ITZ refinement and left the matrix more porous. Such performance aligns with the study [17], who emphasized that a polymer alone cannot ensure optimal bonding without adequate mineral admixture integration.

In contrast, M8 achieved the highest slant shear strength (9.1 MPa at 90 days), followed closely by M7 (8.9 MPa) and M9 (8.8 MPa). These mixes contained higher proportions of silica fume and GGBS, which refined the ITZ, reduced porosity, and stimulated secondary C-S-H formation, thereby improving cohesion across the repair interface. Polymer (5%) further strengthened adhesion by penetrating microcracks and forming a continuous polymeric network that anchored the cement paste to the substrate. This mechanism is consistent with Shill et al. [19] and Liang et al. [20], who reported that polymer-SCM systems exhibit superior resistance to delamination and shear failure. Moreover, polypropylene fibers contributed indirectly by controlling crack initiation and restraining stress concentration along the interface, supporting long-term bond stability [23].

Intermediate mixes (M4-M6) demonstrated moderate

strengths (8.4-8.7 MPa at 90 days), indicating that incremental increases in SCM dosage progressively improved interfacial performance. Overall [24], the results confirm that the integration of SCMs, polymer, and fibers generates a denser microstructure, refined ITZ, and stronger chemical and mechanical adhesion, producing a synergistic improvement in slant shear strength compared to polymer-only repair concretes [24, 25].

## 6. CONCLUSIONS

The experimental evaluation of high-performance polymer repair concrete (HPPRC) incorporating sulfate-resisting cement (SRC), SCMs such as silica fume and GGBS, polymer resin (5%), and 0.2% polypropylene fibers has demonstrated notable improvements in mechanical and durability-related properties across all tested parameters. The outcomes rely on how well polymers and SCMs work together to enhance concrete's performance and qualify it for structural repair in harsh environments.

(1) Results for compressive strength showed a steady increase from 28 to 90 days for all mixtures, with the highest strength of 30.1 MPa (M8). This suggests that SCMs are involved over the long term, and polymer has a matrix-densifying and crack-bridging effect. Increased SCM content also improved flexural strength; M8 gained the most at 4.51 MPa, demonstrating the advantages of fiber reinforcement and better ITZ in withstanding tensile stresses.

(2) The polymer's bonding ability and the pore refinement from SCMs were largely responsible for the improved adhesion and cohesion between new and old concrete surfaces, as evidenced by the slant shear strength, a crucial indicator of bond quality in repair applications, which showed values up to 9.03 MPa. The mixtures' suitability for overlays and patching in structural repair scenarios is confirmed by these results. As SCM and polymer content increased, durability metrics like water absorption trended downward. The hypothesis that impermeability is greatly increased by the combination of matrix densification from pozzolanic activity and the polymer's sealing ability was supported by the lowest absorption value of 3.61%. Accordingly, density values increased with better packing density and lower void content from optimized SCM proportions, ranging from 2345 to 2419 kg/m³.

(1) The slump test confirmed that all mixes maintained good workability, with results between 11.1 cm and 12.6 cm, which are well-suited for practical application without segregation. Even with the presence of fibers, the workability was acceptable, demonstrating the mix design’s balance between performance and placement ease.

(2) The synergy between polymer, SCMs, and fibers in the SRC-based HPPRC system resulted in improved mechanical strength, bond performance, reduced porosity, and consistent workability, fulfilling the primary objectives of this research in producing a durable and effective repair concrete system.

The authors declare that there is no conflict of interest regarding the publication of this paper. This research did not receive any specific grant from funding agencies in the public, commercial, or not-for-profit sectors. The authors’ institutional affiliations did not influence the study design, data collection, analysis, or interpretation of results.

## REFERENCE

[1] Xia, P., Khan, S., Hassam, M., Sohaib, M., Gong, F., Zhao, Y. (2024). Optimal utilization of low-quality construction waste and industrial byproducts in sustainable recycled concrete. Construction and Building Materials, 428: 136362. https://doi.org/10.1016/j.conbuildmat.2024.136362

[2] Yuan, P., Zhang, B., Yang, Y., Jiang, T., Li, J., Qiu, J., He, H. (2023). Application of polymer cement repair mortar in underground engineering: A review. Case Studies in Construction Materials, 19: e02555. https://doi.org/10.1016/j.cscm.2023.e02555

[3] Idrees, M., Akbar, A., Saeed, F., Saleem, H., Hussian, T., Vatin, N.I. (2022). Improvement in durability and mechanical performance of concrete exposed to aggressive environments by using polymer. Materials, 15(11): 3751. https://doi.org/10.3390/ma15113751

[4] Kiruthika, C., Prabha, S.L., Neelamegam, M. (2021). Different aspects of polyester polymer concrete for sustainable construction. Materials Today: Proceedings, 43: 1622-1625. https://doi.org/10.1016/j.matpr.2020.09.766

[5] Xie, J., Wang, J., Rao, R., Wang, C., Fang, C. (2019). Effects of combined usage of GGBS and fly ash on workability and mechanical properties of alkali activated geopolymer concrete with recycled aggregate. Composites Part B: Engineering, 164: 179-190. https://doi.org/10.1016/j.compositesb.2018.11.067

[6] Alhazmi, H., Shah, S.A.R., Anwar, M.K., Raza, A., Ullah, M.K., Iqbal, F. (2021). Utilization of polymer concrete composites for a circular economy: A comparative review for assessment of recycling and waste utilization. Polymers, 13(13): 2135. https://doi.org/10.3390/polym13132135

[7] ASTM International. (2022). ASTM C150/C150M-22: Standard specification for portland cement. ASTM International. https://doi.org/10.1520/C0150_C0150M-22

[8] ASTM International. (2022). ASTM C989/C989M-22: Standard specification for (GGBS) cement for use in concrete and mortars. ASTM International. https://doi.org/10.1520/C0989_C0989M-22

[9] ASTM International. (2020). ASTM C881/C881M-20: Standard specification for polymer-resin-base bonding systems for concrete. ASTM International. https://doi.org/10.1520/C0881_C0881M-20

[10] ASTM International. (2023). ASTM C1116/C1116M-23: Standard specification for fiber-reinforced concrete. ASTM International. https://doi.org/10.1520/C1116_C1116M-23

[11] ASTM International. (2018). ASTM C33/C33M-18: Standard specification for concrete aggregates. ASTM International. https://doi.org/10.1520/C0033_C0033M-18

[12] ASTM International. (2020). ASTM C143/C143M-20: Standard test method for slump of hydraulic-cement concrete. ASTM International. https://doi.org/10.1520/C0143_C0143M-20

[13] British Standards Institution (BSI). (2019). BS EN 12390-3:2019: Testing hardened concrete – Part 3: Compressive strength of test specimens. BSI Standards Limited.

[14] ASTM International. (2018). ASTM C78/C78M-18:

Standard test method for flexural strength of concrete (using simple beam with third-point loading). ASTM International. https://doi.org/10.1520/C0078_C0078M-18

[15] ASTM International. (2021). ASTM C882/C882M-13a (2021): Standard test method for BOND strength of polymer-resin systems used with concrete by slant shear. ASTM International. https://doi.org/10.1520/C0882_C0882M-13AR21

[16] ASTM International. (2021). ASTM C642-21: Standard test method for density, absorption, and voids in hardened concrete. ASTM International. https://doi.org/10.1520/C0642-21

[17] Tan, Y., Chen, H., Wang, Z., Xue, C., He, R. (2019). Performances of cement mortar incorporating superabsorbent polymer (SAP) using different dosing methods. Materials, 12(10): 1619. https://doi.org/10.3390/ma12101619

[18] Guo, S.Y., Zhang, X., Chen, J.Z., Mou, B., et al. (2020). Mechanical and interface bonding properties of epoxy resin reinforced Portland cement repairing mortar. Construction and Building Materials, 264: 120715. https://doi.org/10.1016/j.conbuildmat.2020.120715

[19] Shill, S.K., Al-Deen, S., Ashraf, M., Hutchison, W., Hossain, M.M. (2020). Performance of amine cured epoxy and silica fume modified cement mortar under military airbase operating conditions. Construction and Building Materials, 232: 117280. https://doi.org/10.1016/j.conbuildmat.2019.117280

[20] Liang, L., Chen, L., Wu, L., Tan, H. (2021). Interface strength, damage and fracture between ceramic films and metallic substrates. Materials, 14(2): 353. https://doi.org/10.3390/ma14020353

[21] Abed, J.M., Al-Gburi, M., Almssad, A. (2024). Evaluation of physical and mechanical properties of modified cement-lime mortar containing recycled granite powder waste as a partial fine aggregate replacement. Applied Sciences, 14(22): 10146. https://doi.org/10.3390/app142210146

[22] Al-Gburi, M., Abed, J., Almssad, A., Alhayani, A.A., Jędrzejewska, A., Nilsson, M. (2025). The effect of real curing temperatures on early age concrete strength development in massive concrete structures. European Journal of Environmental and Civil Engineering, 29(9): 1832-1847. https://doi.org/10.1080/19648189.2025.2458294

[23] Nichols, K.A., Hu, S.X., White, A.J., Shaffer, N.R., et al. (2024). Time-dependent density-functional theory study on nonlocal electron stopping for inertial confinement fusion. Physics of Plasmas, 31(6): 1-12. https://doi.org/10.1063/5.0201735

[24] Khalil, M.F., Dawood, E.T. (2023). The effects of using eco-friendly materials for the production of high strength mortar. NTU Journal of Engineering and Technology, 2(3): 17-26. https://doi.org/10.56286/ntujet.v2i3.612

[25] Taha, A.R., Al-Attar, A.A., Ahmed, H.M. (2023). The effect of different design ratios on the compressive strength of geopolymer concrete: A parametric study using the Taguchi method. NTU Journal of Engineering and Technology, 2(4): 1-11. https://doi.org/10.56286/ntujet.v2i4.682